Laplacian reconstruction of one single hologram using two different reconstruction distances or wavelengths

Chao Zuo (左 超)***, Qian Chen (陈 钱), Guohua Gu (顾国华), Xiubao Sui (隋修宝), and Jianle Ren (任建乐)**

National Defense Key Laboratory of Optoelectronic Engineering,

Nanjing University of Science and Technology, Nanjing 210094, China

**Corresponding author: surpasszuo@163.com*

A novel numerical algorithm is proposed to reconstruct the Laplacian of an object field from one single in-line hologram. This method uses two different reconstruction distances of z and $z+\Delta z$, or two different reconstruction wavelengths of λ and $\lambda+\Delta\lambda$ to reconstruct one digital in-line hologram. Theoretical analysis shows that when the value of Δz or $\Delta\lambda$ is sufficiently small, the difference of the two reconstructed fields is an approximation to the second-order Laplacian differentiation of the object wave, and the zero-order and "twin-image" noise can be almost eliminated simultaneously. Computer numerical simulations and optical experiments are carried out to validate the effectiveness of this algorithm.

OCIS codes: 090.1995, 050.1970, 110.3010, 100.2980.

doi: 10.3788/COL201210.S10901.

Since the development of high resolution cameras and computer techniques, digital holography has been widely applied to many different fields, such as microscopy[1], particle image velocimetry[2], and deformation analysis[3]. Compared with the conventional holographic technique, numerical reconstruction offers various possibilities for information recovery. Two forms of digital holographic recording are in-line and off-axis. Given the angle between the reference and object beams, digital holograms recorded using off-axis geometry do not fully utilize the available space-bandwidth product of the CCD[4]. In-line architecture remains the mode of choice in many cases, with method phase retrieval[5] or phase shifting[6] being used for reconstruction.

Methods of differential reconstruction of an optical wave field have recently been proposed, which differ from the direct reconstruction of the original object wave field[7−9]. The spatial derivative of an optical wave field can be used for enhancing the edges of objects, automatic focusing, and holographic reconstruction of three-dimensional objects[10]. It has been shown that, by Fresnel propagating the difference of two such holograms, recorded at two displaced planes[7,8] or with different wavelengths[9], the resultant reconstruction is an approximation to the Laplacian second order differentiation of the object wave field.

In this letter, a new algorithm to realize the Laplacian differential reconstruction of an optical wave field is presented. This method only needs one in-line digital hologram captured at a certain distance with a certain wavelength by CCD, then uses two different distances or wavelengths to reconstruct it. By subtracting the two reconstructed wave fields, the result is approximately equal to the Laplacian second-order differentiation of the object wave in the transverse direction. The principles, simulations, and experimental results are explained below.

The basic principle of in-line holography recording is illustrated using the schematic shown in Fig. 1. The intensity of the incident coherent beam, diffracted when crossing the object and free propagated beyond is recorded on the digital camera. The reference and the object waves

are not separate beams, but a unique one. This simplified recording setup gives a good stability in adequation with industrial application constraints.

Suppose the complex-amplitude distribution of the object wave in the object plane (corresponding to $z = 0$ in the z axis) is $o(x, y, 0)$. The resulting interference pattern is recorded at the camera plane located at a distance of z from the object plane. The intensity hologram pattern can be written in the form of

$$I(x,y,z) = |r(x,y)|^2 + |o(x,y,z)|^2 \\ + r(x,y)o^*(x,y,z) + r^*(x,y)o(x,y,z), \quad (1)$$

where $r(x,y)$ stands for the reference plane wave, and $o(x,y,z)$ is the diffraction patterns of the object $o(x,y,0)$ at the recording plane z. The object wave fields $o(x,y,z)$ can be expressed using the scalar diffraction theory as

$$o(x,y,z) = F^{-1}\left\{O(\xi,\eta,0)\exp\left[\mathrm{i}2\pi z\sqrt{\frac{1}{\lambda} - (\xi^2+\eta^2)}\right]\right\}. \quad (2)$$

where F^{-1} represents the inverse Fourier transform operation, and $O(\xi,\eta,0)$ denotes the Fourier transform of $o(x,y,0)$. In the Fresnel paraxial approximation, Eq. (2) can be simplified as

$$o(x,y,z) = \exp\left(\mathrm{i}\frac{2\pi}{\lambda}z\right) \\ \cdot F^{-1}\left\{O(\xi,\eta,0)\exp\left[\mathrm{i}\pi\lambda z\left(\xi^2+\eta^2\right)\right]\right\}. \quad (3)$$

Let us assume that the hologram reconstruction is achieved by illumination with plane-wave reference, as with classical holography. This process now could be modeled numerically by propagating from the camera
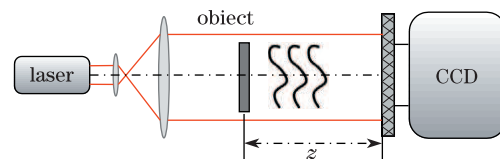

Fig. 1. In-line digital holography setup.

recording plane a distance $-z$ back to the object plane.

$$Df_{-z}(I) = \text{DC} + r(x,y)o^*(x,y,2z) + r^*(x,y)o(x,y,0), \tag{4}$$

where $Df_{-z}(I)$ denotes the inverse diffraction integration through the distance of $-z$. Obviously, the reconstruction field includes three parts: The DC term on the right-hand side of Eq. (4) is the zero order of diffraction equal to $|r(x,y)|^2 + |o(x,y,0)|^2$. The second term in Eq. (4) produces a real image located on the other side of the hologram, whereas the third term produces a virtual image located at the position initially occupied by the object.

If we change the distance of numerical inverse diffraction from z to $z + \Delta z$, another diffraction field $Df_{-(z+\Delta z)}(I)$ near the object plane can be obtained. We then calculate the difference between $Df_{-z}(I)$ and $Df_{-(z+\Delta z)}(I)$:

$$\begin{aligned}
\Delta Df_z(I) =& Df_{-z}(I) - Df_{-(z+\Delta z)}(I) \\
=& \Delta Df_z(\text{DC}) + r(x,y)\exp\left(\mathrm{i}\frac{2\pi}{\lambda}z\right) \\
& \cdot F^{-1}\left\{O^*(-\xi,-\eta,0)\exp\left[\mathrm{i}2\pi\lambda z\left(\xi^2+\eta^2\right)\right]\right. \\
& \cdot\left\{1 - \exp[\mathrm{i}\pi\lambda\Delta z\left(\xi^2+\eta^2\right)]\right\}\} \\
& + r^*(x,y)\exp\left(\mathrm{i}\frac{2\pi}{\lambda}z\right) \\
& \cdot F^{-1}\{O(\xi,\eta,0)\{1-\exp\left[\mathrm{i}\pi\lambda\Delta z\left(\xi^2+\eta^2\right)]\}\}.
\end{aligned} \tag{5}$$

When the difference between two reconstruction distances Δz is sufficiently small, we can use the Taylor series expansion of $\mathrm{e}^x = \sum_{n=0}^{+\infty}\frac{x^n}{n!}$. Omitting all but the constant and the linear terms gives

$$\exp\left[\mathrm{i}\pi\lambda\Delta z\left(\xi^2+\eta^2\right)\right] \cong 1 + \mathrm{i}\pi\lambda\Delta z\left(\xi^2+\eta^2\right). \tag{6}$$

Note: This approximation is applicable as long as the quadratic term in the Taylor expansion $\frac{1}{2}\left[\mathrm{i}\pi\lambda\Delta z\left(\xi^2+\eta^2\right)\right]^2$ is much less than one. Furthermore, the difference of the DC terms $\Delta Df_z(\text{DC})$ is negligible and can be omitted from Eq. (5). Substituting Eq. (6) into Eq. (5) and neglecting the phase:

$$\begin{aligned}
\Delta Df_z(I) =& -\mathrm{i}\pi\lambda\Delta z r(x,y)F^{-1}\left\{\left(\xi^2+\eta^2\right)O^*(-\xi,-\eta,0)\right. \\
& \cdot \exp\left[\mathrm{i}2\pi\lambda z\left(\xi^2+\eta^2\right)\right]\} - \mathrm{i}\pi\lambda\Delta z r^*(x,y) \\
& \cdot F^{-1}\left\{\left(\xi^2+\eta^2\right)O(\xi,\eta,0)\right\}.
\end{aligned} \tag{7}$$

According to the differential properties of Fourier transform, we have

$$\begin{aligned}
\Delta Df_z(I) =& \frac{\mathrm{i}\lambda\Delta z}{4\pi}r(x,y)\nabla^2_{xy}o^*(x,y,-2z) \\
& + \frac{\mathrm{i}\lambda\Delta z}{4\pi}r(x,y)^*\nabla^2_{xy}o(x,y,0).
\end{aligned} \tag{8}$$

When z is a greater distance, for an ordinary object wave, its differential in transverse direction on the object plane is generally much bigger than its differential on the plane $2z$ away from object plane[7]. Thus, the difference of two reconstructed diffraction fields using a differential distance Δz is an approximation to the Laplacian of the object wave.

$$\Delta Df_z(I) \approx \frac{\mathrm{i}\lambda\Delta z}{4\pi}r^*(x,y)\nabla^2_{xy}o(x,y,0). \tag{9}$$

Alternatively, if we use two different wavelengths λ and $\lambda + \Delta\lambda$ to reconstruct the digital hologram and assume that $\Delta\lambda$ is very small, we can also get the Laplacian of the object field:

$$\Delta Df_\lambda(I) \approx \frac{\mathrm{i}z\Delta\lambda}{4\pi}r^*(x,y)\nabla^2_{xy}o(x,y,0). \tag{10}$$

Equation (10) is directly analogous to Eq. (9). Therefore, reconstructing one hologram using two different wavelengths (separated by $\Delta\lambda$), and taking their difference provide an approximation to the Laplacian of the original object field. The two results are in complete accordance with the two-plane[7] and the two-wavelength[9] methods.

The new algorithm is first tested by computer simulation. The synthetic object studied is an opaque letter "A" in a transparent screen of area 0.5×0.5 (mm) with 512×512 pixels. The object is illuminated with a plane wave, of wavelength 632.8 nm, which propagates to the hologram plane at a distance $z = 200$ mm, at normal incidence. The part of the incident light scattered by the object is the object wave and the remainder that does not undergo scattering acts as the reference wave. The hologram plane is of the same size and pixel count as the object plane, and the propagation of optical field is calculated from the Huygens convolution integral[10]. The corresponding computed hologram is the intensity of the diffraction pattern on the hologram plane (Fig. 2(a)).

Figure 2(b) shows the normalized amplitude distribution of directly reconstructed fields by back propagating the holographic image data of Fig. 2(a) from the holograph plane to the object plane. Given the in-line geometry of the setup, the zero-order and the twin images are superposed, and the intensity distribution of the reconstructed field shows clear diffractive patterns of the object, instead of the uniform background. In Fig. 2(c), the normalized magnitude of the Laplacian reconstruction $\Delta Df_z(I)$ using two different reconstruction distances $z = 200$ mm and $z + \Delta z = 201$ mm is given. Similarly, the normalized magnitude of the Laplacian reconstruction $\Delta Df_\lambda(I)$ using two different reconstruction wavelengths $\lambda = 632.8$ nm and $\lambda + \Delta\lambda = 635$ nm is presented in Fig. 2(d). The shape of the object is clearly outlined, and the zero order and twin-image noise effect can hardly be seen in the Laplacian reconstruction images.

To verify the relationship between the magnitude of the Laplacian object field and the differential distance Δz or wavelength $\Delta\lambda$, two sets of Laplacian images were reconstructed using different Δz and $\Delta\lambda$, respectively. The averaged intensities of the Laplacian images are used for quantitative analyses. To better extract the magnitude of the Laplacian object wave field while excluding the large number of pixels with a small magnitude, only those pixels with an intensity larger than the averaged intensity of the whole reconstructed image are taken

into account. The averaged intensities of Laplacian images are shown in Figs. 3(a) and (b) by varying the differential distance Δz and wavelength $\Delta \lambda$. When Δz is less than 10^{-3} m, the relation between the magnitude of the Laplacian object field and the differential distance Δz is approximately linear. When Δz becomes larger, the approximation of Eq. (6) is no longer applicable, which introduces this deviation from linearity. We could get a similar relation in the case of different reconstruction wavelengths. These results are consistent with the aforementioned theoretical analysis.

Experiments are also carried out with the setup shown in Fig. 1 to demonstrate the validation of this method. The semiconductor laser diode used in the experiment was an InGaP type with a wavelength of 635 nm and output power of 3 mW. The point part of a needle positioned at $z = 175$ mm was illuminated by the collimated beam. Diffraction intensity pattern was recorded with a CCD camera with $1\,024 \times 1\,024$ pixels, with a pixel size of 5.5 μm. The recorded hologram and its corresponding directly reconstructed image are shown in Figs. 4(a) and (b). The magnitude of the Laplacian reconstruction using two different distances and wavelengths are shown in Figs. 4(c) and (d), respectively. Perfect Laplacian second-order differentiation reconstruction cannot be achieved in the presence of noise[11,12]. However, the object edge can be clearly identified despite some noise in the two Laplacian images, demonstrating the effectiveness of our approach. Moreover, the signal-to-noise ratio of the Laplacian images can be improved using speckle reduction methods[13].

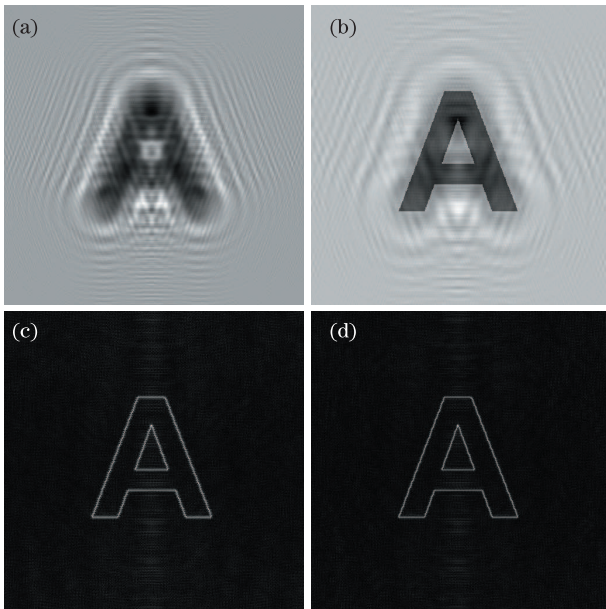This experiment was also repeated using different reconstruction distances and wavelengths, and
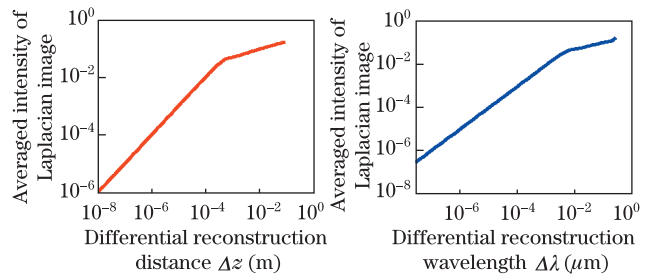

Fig. 3. Averaged intensity of Laplacian image versus (a) differential reconstruction distance and (b) differential reconstruction wavelength.
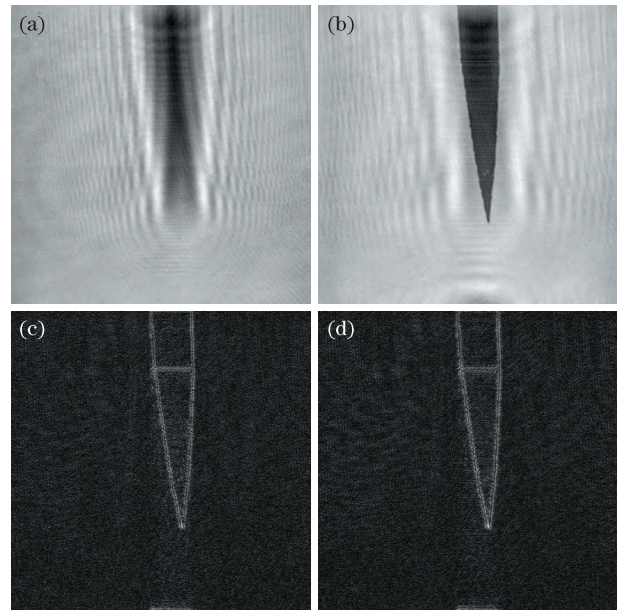

Fig. 4. (a) In-line hologram of a needle recorded at $z = 175$ mm. (b) Directly reconstructed image by one hologram shown in (a). (c) Magnitude of Laplacian differential reconstruction using two reconstruction distances of z=175 mm and $z + \Delta z$=178 mm. (d) Magnitude of Laplacian differential reconstruction using two reconstruction wavelengths of $\lambda = 635$ nm and $\lambda + \Delta \lambda = 650$ nm.

the results indicated that: (1) If $\Delta z/z$ is equal to $\Delta \lambda / \lambda$, the two methods (using two reconstruction distances/wavelengths) would give almost the same results. (2) The quality of reconstructed images may degenerate when the value of $\Delta z/z$ (or $\Delta \lambda / \lambda$) is either too small ($<0.5\%$) or too large ($>2\%$). These results are consistent with our theoretical analysis and those in Refs. [7–9].

In conclusion, a new digital holography reconstruction algorithm based on the reconstruction of one in-line hologram using two reconstruction distances or wavelengths is proposed. By the subtraction of the two reconstructed diffraction fields, the Laplacian second-order differentiation of the object wave can be obtained without the zero-order and twin-image noise. The practical advantage of the proposed method is that it requires only one single capture and no additional experimental operation. In addition, the said method can be performed rapidly, and shows results similar to the multiple captures with two-plane or two-wavelength methods. Theoretical analysis, computer simulations, and optical experimental results indicate that it is an effective means to realize the

Fig. 2. (a) Hologram of an opaque letter "A" computer generated. (b) Classical reconstructed image directly by one hologram shown in (a). (c) Magnitude of Laplacian differential reconstruction using two reconstruction distances of z=200 mm and $z + \Delta z$=201 mm. (d) Magnitude of Laplacian differential reconstruction using two reconstruction wavelengths of $\lambda = 632.8$ nm and $\lambda + \Delta \lambda = 635$ nm.

Laplacian differential reconstruction of the object wave using one in-line digital hologram. This algorithm is especially applicable for enhancing the edge information of the object wave and pinpointing the position of the objects, automatically determining the focused image plane in the process of digital reconstruction, recognition, and classification of three-dimensional objects.

References

1. K. J. Chalut, W. J. Brown, and A. Wax, Opt. Express **15,** 3047 (2007).
2. M. Adams, T. M. Kreis, and W. P. O. Juptner, Proc. SPIE **3098,** 234 (1997).
3. G. Pedrini, P. Fröning, H. Tiziani, and F. M. Santoyo, Opt. Commun. **164,** 257 (1999).
4. H. Wang, D. Wang, J. Zhao, and J. Xie, Chin. Opt. Lett. **6,** 165 (2008).
5. G. Liu and P. D. Scott, J. Opt. Soc. Am. A **4,** 159 (1987).
6. I. Yamaguchi and T. Zhang, Opt. Lett. **22,** 1268 (1997).
7. C. S. Guo, Q. Y. Yue, G. X. Wei, L. L. Lu, and S. J. Yue, Opt. Lett. **33,** 1945 (2008).
8. Y. J. Han and Q. Y. Yue, Opt. Commun. **283,** 929 (2010).
9. J. P. Ryle, D. Li, and J. T. Sheridan, Opt. Lett. **35,** 3018 (2010).
10. H. Zheng, T. Wang, L. Dai, and Y. Yu, Chin. Opt. Lett. **9,** 040901 (2011).
11. J. J. Healy and J. T. Sheridan, J. Opt. Soc. Am. A **28,** 786 (2011).
12. D. Li, D. P. Kelly, and J. T. Sheridan, J. Opt. Soc. Am. A **28,** 1896 (2011).
13. D. Li, D. P. Kelly, and J. T. Sheridan, J. Opt. Soc. Am. A **28,** 1904 (2011).
14. W. Xiao, J. Zhang, L. Rong, F. Pan, S, Liu, F. Wang, and A. He, Chin. Opt. Lett. **9,** 060901 (2011).